

## Influence of Substrate Conductivity on Circulation Reversal in Evaporating Drops

W. D. Ristenpart, P. G. Kim, C. Domingues, J. Wan, and H. A. Stone

*School of Engineering and Applied Sciences, Harvard University, Cambridge, Massachusetts 02138, USA*

(Received 12 July 2007; published 3 December 2007)

Nonuniform evaporation from sessile droplets induces radial convection within the drop, which produces the well-known “coffee-ring” effect. The evaporation also induces a gradient in temperature and consequently a gradient in surface tension, generating a Marangoni flow. Here we investigate theoretically and experimentally the thermal Marangoni flow and establish criteria to gauge its influence. An asymptotic analysis indicates that the direction of the flow depends on the relative thermal conductivities of the substrate and liquid,  $k_R \equiv k_S/k_L$ , reversing direction at a critical contact angle over the range  $1.45 < k_R < 2$ . We corroborate the theory experimentally and demonstrate that the Marangoni flow can significantly influence the resulting patterns of particle deposition.

DOI: 10.1103/PhysRevLett.99.234502

PACS numbers: 47.55.pf, 47.55.nb, 82.70.Dd

The hydrodynamic consequences of nonuniform evaporation from sessile droplets are important not only because of their ubiquitous nature (e.g., coffee stains [1]) but also because of the implications for a variety of evaporative self-assembly techniques [2–5] and printing applications [6–8]. Early investigators led by Deegan *et al.* [1,9,10] observed the flow patterns in drops with pinned contact lines and explained the flow in terms of the higher rate of mass loss near the contact line. They also noted, however, that the flow field is affected by surface tension gradients, i.e., Marangoni flows [9]. The nonuniform evaporation draws energy unevenly from the drop, creating temperature gradients and consequently altering the surface tension. Deegan *et al.* assumed that the drop was coldest on top because of the longer conduction path from the isothermal substrate. Although numerical simulations have corroborated this view for evaporating drops on substrates with infinite thermal conductivities [11–13], numerical calculations on a substrate with finite conductivity have suggested the circulation reverses direction at a critical contact angle [14]. This result is both surprising and significant, since Marangoni flow directed radially inward along the substrate actively hinders the deposition of particles at the drop edge. The circulation reversal has not been observed experimentally, however, and despite extensive investigations of the coffee-stain problem [1,9–21] the role of substrate thermal conductivity has remained unclear.

In this Letter we establish quantitative criteria for the magnitude and direction of thermal Marangoni flow inside evaporating sessile drops, and we show that the circulation direction depends on both the contact angle and the ratio of substrate and liquid thermal conductivities. An asymptotic analysis indicates that the drop is warmest at the contact line only if the substrate conductivity  $k_S$  is at least a factor of 2 greater than the liquid conductivity  $k_L$  (i.e.,  $k_R \equiv k_S/k_L > 2$ ). In this situation, the consequent Marangoni flow is directed radially *outward* along the substrate. For  $1.45 < k_R < 2$ , the direction of the temperature gradient (and the resulting flow) depends on the contact angle  $\theta_c$ ,

while for  $k_R < 1.45$  the drop is coldest near the contact line and the circulation direction is reversed, i.e., radially *inward* along the substrate. These predictions are corroborated experimentally using organic liquids on insulating substrates. Furthermore, the experiments confirm that the Marangoni flow, of either direction, significantly alters the resulting particle deposition patterns, an effect with implications for printing applications [7,8], “Marangoni drying” techniques for cleaning substrates [22], and evaporative self-assembly of colloids [23,24].

We focus on slowly evaporating drops in which the mass flux of vapor from the drop is described by

$$j(x) = j_0[1 - (x/R)^2]^{-1/2 + \theta_c/\pi}, \quad (1)$$

where  $\theta_c$  is the contact angle ( $0 < \theta_c < \pi/2$ , cf. Fig. 1),  $x$  is the distance from the center of the drop which has radius  $R$ , and the prefactor  $j_0$  depends on the saturation pressure, the vapor diffusivity, and the far field concentration. Numerical calculations indicate that this expression is accurate to within 5% over the entire range of contact angles [18]. The nonuniform flux induces flow inside drops with pinned contact lines to satisfy conservation of mass, but it also withdraws energy from the system. For negligible heat conduction and convection in the air, the interfacial energy balance is

$$-k_L \mathbf{n} \cdot \nabla T = \Delta H_v j(x) \quad \text{at } y = h(x), \quad (2)$$

where  $\Delta H_v$  is the specific latent heat of evaporation and  $\mathbf{n}$

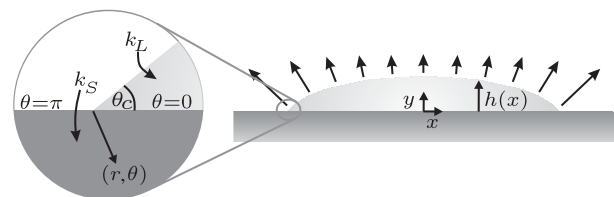


FIG. 1. Sketch of an evaporating liquid drop on a solid substrate, with a magnification of the three-phase contact line.

is the unit normal. Since  $j(x)$  varies with position, the temperature varies, and consequently a gradient in surface tension must be balanced by viscous stress. Accordingly, the tangential stress  $\tau$  is

$$\tau = \mathbf{t} \cdot \nabla_s \gamma = \beta(\mathbf{t} \cdot \nabla_s T) \quad \text{at } y = h(x), \quad (3)$$

where  $\mathbf{t}$  is the tangential unit vector,  $\nabla_s$  is the surface gradient, and  $\beta \equiv \partial\gamma/\partial T$  is a material parameter that is negative for most liquids. In writing the stress in terms of a temperature gradient only, we are assuming that other sources of Marangoni stress, e.g., surfactant concentration gradients, are negligible. Thus, the sign of the temperature gradient at the air/liquid interface governs the direction of circulation in the drop.

To determine the sign of the temperature gradient, in general we must solve for an unknown temperature distribution  $T_0(x)$  at  $y = 0$  which depends on the geometry and material properties of the substrate. To avoid this complication, we instead employ an asymptotic methodology to examine the effect of the flux given by Eq. (1) on heat transfer in the immediate vicinity of the three-phase contact line. Although this approach does not yield a solution throughout the drop, it does provide a means to determine the direction of the temperature gradient and consequently the Marangoni flow.

The three-phase contact line is sketched in Fig. 1. Very close to the contact line, the curvature of the drop surface is negligible so the interface may be modeled as a straight line emanating from the solid substrate at an angle  $\theta_c$ . In this configuration it is convenient to choose cylindrical coordinates  $(r, \theta)$ . Upon substitution of  $x/R = 1 - r \cos\theta_c$ , the expansion around  $r = 0$  is

$$j(r) = j_0(2r \cos\theta_c)^{-1/2+\theta_c/\pi} + \dots \quad (4)$$

To examine the consequences of Eq. (4) on the temperature distribution, we assume that the transport is quasi-steady. The thermal energy equation is then  $\text{Pe} \mathbf{u} \cdot \nabla T = \nabla^2 T$ , where the Peclet number  $\text{Pe}$  gauges the relative magnitudes of convective and conductive heat transfer. Typically  $\text{Pe} \ll 1$ , but as originally pointed out by Deegan *et al.*, the velocity due to mass loss diverges in the local vicinity of the contact line [1]. Although this raises the possibility that convection dominates the heat transfer in the corner, it is straightforward to show that conduction is nonetheless dominant [25].

The temperature is thus governed by Laplace's equation  $\nabla^2 T = 0$ , and the temperature fields are given by  $T_i = r^\lambda [A_i \cos(\lambda\theta) + B_i \sin(\lambda\theta)]$ . Here  $i = L, S$  for the liquid and substrate, respectively, and the constants  $\lambda$ ,  $A_i$ , and  $B_i$  must be determined. Four boundary conditions are required. At the solid/air interface ( $\theta = \pi$ ), we assume that conduction in the air is negligible so the heat flux is zero,  $\mathbf{n} \cdot \nabla T_S = 0$ . At the drop-solid interface ( $\theta = 0$ ) we require continuity of temperature,  $T_L = T_S$ , and continuity of the heat flux,  $k_L \mathbf{n} \cdot \nabla T_L = k_S \mathbf{n} \cdot \nabla T_S$ . The final boundary condition at  $\theta = \theta_c$  is obtained by using Eq. (4) in

Eq. (2). Matching the powers of  $r$  shows that  $\lambda = 1/2 + \theta_c/\pi$ , and application of the four boundary conditions yields the constants  $A_i$  and  $B_i$  [25]. Note that this procedure does not yield the absolute temperature, since only fluxes are specified at the boundaries, but this is unimportant since the Marangoni stress is proportional to the temperature gradient. Also note that the solution is valid for all contact angles  $0 < \theta_c < \pi/2$ .

Isotherms are presented for different values of  $k_R$  in Fig. 2. The results indicate that for  $k_R \gg 1$  the heat flux at the liquid/substrate interface is predominantly normal to the substrate, while for  $k_R \sim 1$  the flux has a significant tangential component. To understand the physical significance of this result, it is fruitful to think in terms of the availability of energy from the substrate. Recall that the heat flux from the drop is largest near the contact line. For substrates with large thermal conductivities, energy is readily supplied to the contact line region, so the interface is able to maintain a comparatively high temperature despite the energy lost to evaporation. In this situation the conduction through the drop is dominant, and the drop is warmest near the contact line. In contrast, energy is not readily available for substrates with low thermal conductivities. In this case, energy is extracted from the drop itself and consequently the edge of the drop is coldest.

With respect to Marangoni flow, the circulation direction is controlled by the temperature gradient at  $\theta = \theta_c$ , which from the asymptotic corner solution is

$$\left. \frac{\partial T_L}{\partial r} \right|_{\theta=\theta_c} = C r^{\lambda-1} \left( \frac{1 + k_R \tan(\lambda\pi) \tan(\lambda\theta_c)}{\tan(\lambda\theta_c) - k_R \tan(\lambda\pi)} \right), \quad (5)$$

where  $C \equiv \Delta H_v j_0 / k_L (2 \cos\theta_c)^{\lambda-1}$ . Given that  $0 < \theta_c < \pi/2$  and  $\lambda = 1/2 + \theta_c/\pi$ , the inequalities  $\lambda > 1/2$  and  $\lambda\theta_c < \pi/2$  are satisfied. Hence, the direction of the temperature gradient depends only on the sign of the numerator,  $1 + k_R \tan(\lambda\pi) \tan(\lambda\theta_c)$ . For sufficiently large values of  $k_R$ , the numerator is negative and the temperature decreases with distance from the contact line. For  $\beta < 0$ , Eq. (3) indicates that the resulting Marangoni flow will be directed radially *inward* along the air-liquid interface, and

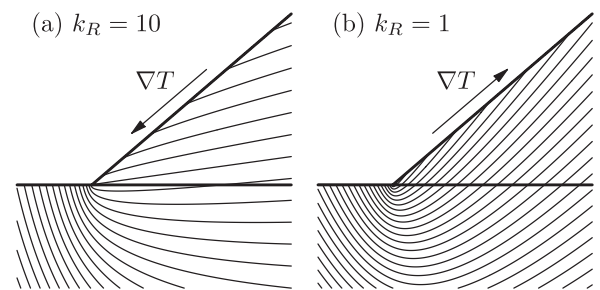


FIG. 2. Asymptotic temperature distributions near the contact line of an evaporating drop with  $\theta_c = \pi/8$  (not to scale). Arrows indicate direction of increasing temperature. (a) Isotherms for  $k_R = 10$ . The heat flux is approximately normal to the substrate. (b) Isotherms for  $k_R = 1$ . The heat flux has a large component tangential to the substrate.

consequently radially *outward* along the liquid-solid interface. If the thermal conductivity of the substrate is below a critical value, however, then the temperature increases with distance. In this situation, the drop is coldest at the edge of the droplet, rather than the top, and the direction of the flow is reversed. The critical thermal conductivity ratio obtained by setting Eq. (5) to zero is

$$k_R^{\text{crit}} = \tan(\theta_c) \cot\left(\frac{\theta_c}{2} + \frac{\theta_c^2}{\pi}\right), \quad (6)$$

which is plotted in Fig. 3. For values of  $k_R$  above (below) the curve, the temperature decreases (increases) with distance from the contact line, and the flow is directed radially outward (inward) along the substrate. Note that for  $k_R < 1.45$  and  $k_R > 2$  the circulation direction is insensitive to the contact angle. However, a wide range of liquids have thermal conductivities comparable to many commonly used plastics and inorganic materials. For example, water and glass have  $k_R \approx 1.6$ , and according to Eq. (6) the Marangoni flow reverses direction at  $\theta_c = 0.54$  ( $31^\circ$ ). This result is consistent with the numerical work by Hu and Larson [14], who found that the flow reversed direction at  $\theta_c = 14^\circ$  (triangles, Fig. 3).

To further test the validity of Eq. (6) as a criterion for the direction of circulation, we performed a series of experi-

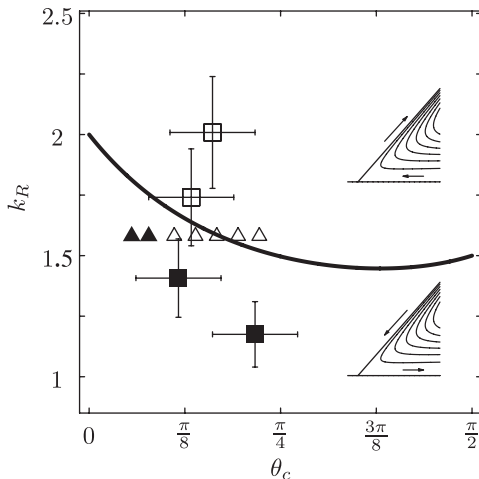


FIG. 3. Experimental observations and numerical calculations of the circulation direction inside evaporating drops. The solid black line is Eq. (6). Regions above and below the line correspond to circulation directions sketched in the respective streamlines (insets), obtained from the asymptotic corner flow solution [25]. Open symbols: observed direction of circulation consistent with temperature decreasing with distance from the contact line. Filled symbols: reverse circulation observed, consistent with temperature increasing with distance from the contact line. Triangles: numerical calculations by Hu and Larson for water on glass [14]. Squares: experimental observations for various liquids on PDMS. From top to bottom: chloroform, isopropanol, ethanol, and methanol. Error bars represent uncertainty in thermal conductivity measurements and the dynamic contact angle during evaporation.

ments with different volatile liquids on polydimethylsiloxane (PDMS) substrates. PDMS is convenient because of its low thermal conductivity ( $k_S = 0.23 \pm 0.03 \text{ W m}^{-1} \text{ K}^{-1}$ , measured with an axial heat flux method [26]), and because many fluids are partially wetting on it. To trace the flow, polystyrene particles  $1 \mu\text{m}$  in diameter were suspended at roughly 0.1% volume fraction in separate solutions of methanol, ethanol, and isopropanol;  $1 \mu\text{m}$  silica particles were similarly suspended in chloroform. PDMS slabs 4 mm thick were rigorously cleaned and dried with compressed air, then individual  $2 \mu\text{L}$  drops of solution were placed on the PDMS and allowed to evaporate. The resulting flow was observed from below with an optical microscope. Adjusting the focal plane of the microscope vertically allowed visualization of the radial component of the particle motion at different heights in the drop and thus allowed us to discern the direction of circulation. The PDMS and drop were placed inside a large covered petri dish to minimize disturbances from air currents.

For each fluid tested, the first 30 to 60 seconds after placement of the drop were characterized by rapid chaotic motion, followed by a rapid transition to a slower, more orderly axisymmetric flow. The driving force for the chaotic flow is unclear; one possibility is the Bénard-Marangoni instability [27]. Nonetheless, the subsequent axisymmetric flow is consistent with flow due to thermal Marangoni stress at the air/liquid interface; approximate streamlines for the observed flow are depicted in Fig. 4(a). Although the streamlines presented in Fig. 4(a) were calculated by means of a lubrication analysis [25] for thermal Marangoni flow on a conductive substrate ( $k_R \gg 1$ ), they qualitatively capture the shape of the experimentally observed flow on an insulating substrate. This suggests that the shape of the Marangoni flow is qualitatively similar for both conducting and insulating substrates.

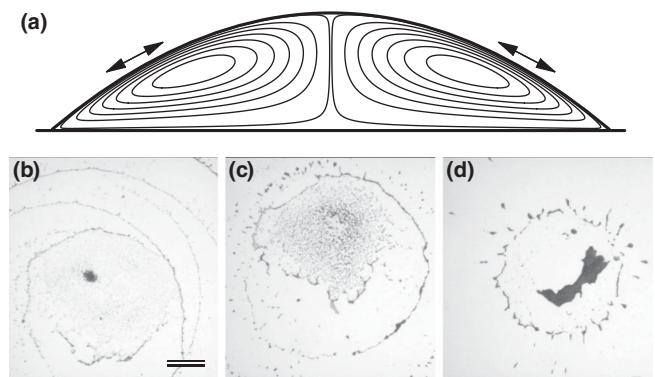


FIG. 4. (a) Qualitative depiction of the streamlines observed inside evaporating droplets on PDMS. Arrows indicate the direction of circulation for different liquids: upward for isopropanol and chloroform, downward for methanol and ethanol. (b)–(d) Particle deposition patterns resulting from different evaporating fluids on PDMS. In each case, a high concentration of particles deposited in a central part of the pattern near the stagnation points of the Marangoni flow. (b) Methanol. (c) Ethanol. (d) Isopropanol. Scale bar is 0.2 mm.

The key result, however, is that the direction of circulation varied among the different liquids and was correlated with the thermal conductivity. For methanol and ethanol ( $k_R = 1.1$  and  $1.4$ , respectively), the particle motion was observed to be radially *inward* along the substrate and radially *outward* along the air/liquid interface, consistent with Marangoni flow induced by a positive temperature gradient along the air/liquid interface (cf. Figure 3, filled squares). We emphasize that the motion along the substrate is in the direction opposite of that expected due to mass loss at the contact line (i.e., in the coffee-ring flow [1]). In contrast, for isopropanol and chloroform ( $k_R = 1.7$  and  $2.0$ , respectively) the observed circulation was radially outward along the substrate and radially inward along the air/liquid interface, again consistent with the theory (cf. Fig. 3, open squares).

The experiments also indicated that Marangoni flow of either direction has a pronounced but similar impact on the resulting particle deposition patterns [Fig. 4(b)–4(d)]. In the liquids studied here, some fraction of the particles accelerated into and then adhered to the substrate at the contact line, in a manner similar to that observed in the coffee-ring problem [1]. Most particles, however, failed to reach the contact line, at first approaching it and then moving away in a manner consistent with the inset streamlines in Fig. 3. A fraction of the recirculating particles tended to subsequently collect at the stagnation points near the center of the drop (either near the air/liquid interface or near the substrate). As the drop evaporated, the particles near the stagnation points remained near the center of the drop, as evidenced by the high concentration of particles near the center of the dry patterns shown in Fig. 4(b)–4(d). A similar observation was reported previously [20] for the case of Marangoni flow directed radially outward along the substrate (octane on glass,  $k_R \approx 8$ ); our results show that Marangoni flow directed in either direction ultimately forces particles toward the center. Aside from the similar feature of extensive deposition near the center, however, the detailed structures of the deposition patterns vary significantly. This observation suggests that the final pattern depends on a sensitive balance of colloidal and capillary interactions during the final stages of evaporation. Nonetheless, the Marangoni flows studied here clearly affect the deposition patterns by forcing particles toward the drop center. More work will be necessary to establish quantitatively how the direction and magnitude of the Marangoni flow affect the details of the particle deposition process.

In summary, we demonstrated experimentally that thermal Marangoni flow in evaporating droplets depends sensitively on the ratio of thermal conductivities of the liquid and substrate, and we derived quantitative criteria for the circulation direction and magnitude. The present work focused on the case where surfactant gradients are negli-

gible, and the agreement between the theory and experiments for the liquids examined here suggests this assumption is adequate for organic liquids. However, solutal effects are important in other systems [28]; for example, they are believed to suppress thermal Marangoni flow in pure water [14] and to induce strong circulation in certain biological systems where chemotaxis occurs [29]. The theory presented here serves as a framework for addressing these more complicated effects.

We thank Harvard MRSEC (DMR-0213805) and NSF-REU (DMR-0353937) for their support.

- 
- [1] R. D. Deegan *et al.*, Nature (London) **389**, 827 (1997).
  - [2] P. Jiang, J. F. Bertone, K. S. Hwang, and V. L. Colvin, Chem. Mater. **11**, 2132 (1999).
  - [3] E. Rabani *et al.*, Nature (London) **426**, 271 (2003).
  - [4] S. Narayanan, J. Wang, and X. M. Lin, Phys. Rev. Lett. **93**, 135503 (2004).
  - [5] M. Schnell-Levin, E. Lauga, and M. P. Brenner, Langmuir **22**, 4547 (2006).
  - [6] P. Calvert, Chem. Mater. **13**, 3299 (2001).
  - [7] J. Park and J. Moon, Langmuir **22**, 3506 (2006).
  - [8] J. Wang and J. R. G. Evans, Phys. Rev. E **73**, 021501 (2006).
  - [9] R. D. Deegan, Phys. Rev. E **61**, 475 (2000).
  - [10] R. D. Deegan *et al.*, Phys. Rev. E **62**, 756 (2000).
  - [11] R. Savino and S. Fico, Phys. Fluids **16**, 3738 (2004).
  - [12] F. Girard *et al.*, Langmuir **22**, 11 085 (2006).
  - [13] N. Shahidzadeh-Bonn, S. Rafai, A. Azouni, and D. Bonn, J. Fluid Mech. **549**, 307 (2006).
  - [14] H. Hu and R. G. Larson, Langmuir **21**, 3972 (2005).
  - [15] E. Adachi, A. S. Dimitrov, and K. Nagayama, Langmuir **11**, 1057 (1995).
  - [16] L. Shmuylovich, A. Q. Shen, and H. A. Stone, Langmuir **18**, 3441 (2002).
  - [17] B. J. Fischer, Langmuir **18**, 60 (2002).
  - [18] H. Hu and R. G. Larson, J. Phys. Chem. B **106**, 1334 (2002).
  - [19] H. Hu and R. G. Larson, Langmuir **21**, 3963 (2005).
  - [20] H. Hu and R. G. Larson, J. Phys. Chem. B **110**, 7090 (2006).
  - [21] Y. O. Popov, Phys. Rev. E **71**, 036313 (2005).
  - [22] O. K. Matar and R. V. Craster, Phys. Fluids **13**, 1869 (2001).
  - [23] S. G. Yiantsios and B. G. Higgins, Phys. Fluids **18**, 082103 (2006).
  - [24] D. J. Harris *et al.*, Phys. Rev. Lett. **98**, 148301 (2007).
  - [25] See EPAPS Document No. E-PRLTAO-99-072744 for supplementary material. For more information on EPAPS, see <http://www.aip.org/pubservs/epaps.html>.
  - [26] Similar procedure described in ASTM E1225-04.
  - [27] M. F. Schatz and G. P. Neitzel, Annu. Rev. Fluid Mech. **33**, 93 (2001).
  - [28] V. Truskett and K. J. Stebe, Langmuir **19**, 8271 (2003).
  - [29] I. Tuval *et al.*, Proc. Natl. Acad. Sci. U.S.A. **102**, 2277 (2005).